Structural Engineering and Mechanics, *Vol. 55, No. 6 (2015) 1261-1278*
DOI: http://dx.doi.org/10.12989/sem.2015.55.6.1261

Damping of a taut cable with two attached high damping rubber dampers

Viet Hung Cu[*1,2], Bing Han[1a] and Fang Wang[3b]

[1]*School of Civil Engineering, Beijing Jiaotong University, Beijing 100044, China*
[2]*Bridge and Road Faculty, National University of Civil Engineering, Hanoi, Vietnam*
[3]*Engineering Management Center, China Railway Corporation, Beijing 100844, China*

(Received December 7, 2014, Revised July 1, 2015, Accepted September 15, 2015)

Abstract. Due to their low intrinsic damping, stay cables in cable-stayed bridges have often exhibited unanticipated and excessive vibrations which result in increasing maintenance frequency and disruption to normal operations of the entire bridges. Mitigation of undesired cable vibration can be achieved by attaching an external damping device near the anchorage. High Damping Rubber (HDR) dampers have many advantages such as compact size, better aesthetics, easy maintenance, temperature stability, and cost benefits; therefore, they have been widely used to increase cable damping. Although a single damper has been shown to reduce cable vibrations, it is not the most effective method due to geometric constraints. This paper proposes the use of two HDR dampers to improve effectiveness and robustness in suppressing cable vibration. Oscillation parameters of the cable-dampers system were investigated in detail by modeling the stay cable as a taut string and each HDR damper as complex-valued impedance and by using an analytical formulation of the complex eigenvalue problem. The problem of two HDR dampers arbitrarily located along a cable is solved and the solution is discussed. Asymptotic formulas to calculate the damping ratios of the cable with two HDR dampers installed near the anchorage(s) are proposed and compared with the exact solutions. Further, a design example is presented in order to justify the methodology. The results of this study show that when the two HDR dampers are installed close to each other on the same end of the cable, some interaction between the dampers leads to reduced damping ratio. When the dampers are on the opposite ends of the cable, they are effective in increasing damping ratio and can provide better vibration reduction to multiple modes.

Keywords: taut cable; HDR damper; vibration reduction; damping ratio; complex eigenvalue

1. Introduction

In recent years, with the development of advanced materials, design theories, and construction technology, cable stayed bridges are developing rapidly in quantity and span length. Cables are becoming lighter and more flexible, and consequently have less intrinsic damping. Thus, the cables may suffer large amplitude vibrations induced by dynamic excitations such as those caused by

*Corresponding author, Doctoral Research Fellow, Lecturer, E-mail: 13119006@bjtu.edu.cn
[a]Professor, E-mail: bhan@bjtu.edu.cn
[b]Mater of Science, E-mail: 10121293@bjtu.edu.cn

http://www.techno-press.org/?journal=sem&subpage=8 ISSN: 1225-4568 (Print), 1598-6217 (Online)

moving vehicles, wind, and wind and rain combination (Wenzel and Tanaka 2006, Kumarasena *et al*. 2007, Fujino *et al*. 2012). Wind induced cable vibrations can be categorized as vortex shedding, buffeting or galloping. Moreover, the combination of rain and moderate wind can cause high amplitude stay cable vibration at low frequencies (Hikami and Shiraishi 1988, Matsumoto *et al*. 1992). Frequent and excessive cable vibrations necessitate more frequent maintenance and are detrimental to the safety of the entire bridge structures. Consequently, cable vibration control is a serious concern of engineers in the design of new bridges, as well as in the retrofit of existing bridges.

The mitigation of cable vibration is commonly addressed by attaching an external damper, of which High Damping Rubber (HDR) dampers are the most commonly used type. HDR material has the capability to dissipate significant energy; therefore it has been widely used in buildings and bridge bearings for earthquake resistance. In considering the application of HDR dampers for bridge cables, it can be noted that HDR dampers have many advantages compared to other types of damper, such as compact size, better aesthetics, easy maintenance, temperature stability, and cost benefits. An HDR damper may be composed of several rubber pads attached around the cable and placed at the end of the guide tube. It may also be a rubber ring of annular shape placed inside the guide tube. A single HDR damper is commonly used for stay cables of short length; for example, on the Bai Chay Bridge in Vietnam which has a single stay cable plane and a main span length of 435 m, one HDR damper per stay cable is used for cables having a length between about 50 m to 70 m (Freyssinet 2005).

The vibrations of the cable attached with a single HDR damper were studied using empirical formulas by Nakamura *et al*. (1997). The approximate formulas for damping ratios in the first few modes of a stay cable attached with an HDR damper near the end of the cable were proposed by Fujino and Hoang (2008). In fact, the dampers are often attached to the cable near the anchorage due to geometric constraints and thus the maximum modal damping ratio is low. To increase the damping ratio the use of two dampers at different locations was studied. In the Tatara Bridge, a stay cable is attached with two types of damper: an HDR damper was installed near the bridge tower and a pair of viscous dampers was placed near the bridge deck. To reduce wind induced vibration and additional stresses caused by live loads, a combination of HDR bushing and viscous dampers was used in the Tsurumi Tsubasa Bridge (Takano *et al*. 1997). The influence of rubber bushing on stay-cable damper effectiveness was studied by Main and Jones (2003) in which the rubber bushing was modeled as a linear spring (k). Subsequently, the influence of the stiffness of the damper support was studied by Huang and Jones (2011). Two viscous dampers on a single stay cable were studied in detail based on taut string theory and complex mode eigenvalue by Caracoglia and Jones (2007). The combined effects of two viscous dampers and of one viscous damper combined with one HDR damper were analyzed using asymptotic solutions for the first few modes by Hoang and Fujino (2008). Recently, the modal damping ratio and frequency of taut cable with a viscous damper and a spring were analyzed by Zhou *et al*. (2014).

This paper proposes use of two HDR dampers to improve damping ratio of the cable. The vibrations of a stay cable with two HDR dampers attached at different locations are investigated using analytical formulation of the complex eigenvalue problem. This method has been used by many authors in order to study vibrations of a cable with dampers attached, for example, the studies of a taut cable with an attached single viscous damper by Krenk (2000), Main and Jones (2002a, 2002b), Fujino and Hoang (2008) or two viscous dampers by Caracoglia and Jones (2007), Hoang and Fujino (2008). However, most authors used the asymptotic solution to investigate vibrations of a cable-damper system in the first few modes for only damper locations near the ends of the cable.

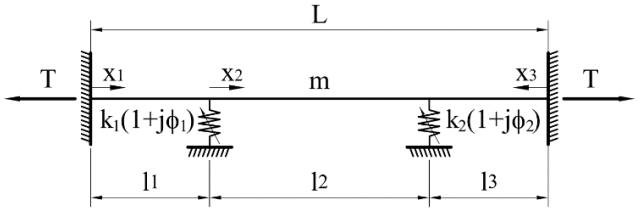

Fig. 1 A model of stay cable with attached two HDR dampers

In this paper, oscillation parameters of the cable-two HDR dampers system are considered in detail through finding the exact values of the complex eigenvalue; thus the restriction on the damper location and mode in the formulation is resolved. Further, this paper also proposes asymptotic formulas for the calculation of damping ratios of a cable when two HDR dampers are installed near the ends of the cable, the accuracy of which is compared with the exact solution.

In elastic materials, force and displacement are linearly related following Hooke's law. However, in real materials such as polymers and elastomers, mechanical responses depend on strain rate and frequency (Jung *et al*. 2006). HDR's behavior has two elements: one is time-independent and the other is time-dependent. The time independent element is the static force-deformation relationship. The time dependent nature is represented by the loss modulus. The complex modulus (E) is represented mathematically by the real part E_1 and the imaginary part E_2 as $E = E_1 + jE_2$ where $j^2 = -1$. The ratio of the loss to the storage modulus is defined as the material loss factor which is determined as $\phi = E_2/E_1 = \tan(\delta)$ with $\tan(\delta)$ being the tangent of the phase angle between stress and strain (Bert 1973). Thus, in this paper, the HDR damper is modeled as complex-valued impedance with spring factor (k) and material loss factor (ϕ). Complex impedance $k(1+j\phi)$ represents a viscous-elastic linear behavior of the HDR damper. Due to the hysteretic properties of the HDR, the damping force can be expressed as $F_d = k(1+j\phi)u_d$ where u_d is transverse motion at the damper location.

This parametric study provides insights into the dynamics of cable-two HDR dampers system and so can act as a tool for evaluating and selecting optimal damper parameters.

2. Motion equation of a stay cable with two attached HDR dampers

A model of a taut cable with two HDR dampers attached is shown in Fig. 1 where k_1 and k_2 are the spring factors, and ϕ_1 and ϕ_2 are the material loss factors of the HDR dampers. Assume the tension force in the cable is large compared to its weight so that the deflection of the cable is small. Influence of bending stiffness and intrinsic mechanical damping of the cable are neglected.

The two dampers divide the cable into three segments. The partial differential equation over each segment of the cable is as below

$$T\frac{\partial^2 u_n(x_n,t)}{\partial x_n^2} = m\frac{\partial^2 u_n(x_n,t)}{\partial t^2} \tag{1}$$

where T is tension in the cable, $u_n(x_n,t)$ is transverse deflection, x_n is coordinate along the cable chord axis in the n^{th} segment, and m is mass per unit length. This equation is valid everywhere except at the damper attachment points, where the continuity of displacements and equilibrium of forces must be

satisfied.

Using Bernoulli method, solution of equation is as follows

$$u_n(x_n,t) = Y_n(x_n)e^{j\omega t} \tag{2}$$

where $Y_n(x_n)$ is complex mode shape on n^{th} cable segment, $j=\sqrt{-1}$ and ω is complex circular frequency of cable.

The dimensionless frequency is defined as $\lambda=\sigma+j\varphi$, leading to $\omega=\lambda\omega_1^0$, where $\omega_1^0=(\pi/L)\sqrt{T/m}$ is natural circular frequency of the first mode.

Substituting Eq. (2) into Eq. (1) yields

$$\frac{d^2Y_n(x_n)}{dx_n^2}+\left(\frac{\pi\lambda}{L}\right)^2 Y_n(x_n)=0 \tag{3}$$

The boundary conditions of zero displacements at the cable ends

$$u_n(0,t)=0; \quad n=1,3 \tag{4}$$

The continuity of displacements of cable at the damper locations

$$u_1(l_1,t)=u_2(0,t)=\gamma_1 \tag{5}$$

$$u_2(l_2,t)=u_3(0,t)=\gamma_2 \tag{6}$$

where γ_q are amplitudes at the dampers.

Enforcing Eqs. (4)-(6), the solution can be expressed in the forms below

$$\begin{cases} Y_1(x_1)=\gamma_1\dfrac{\sin(\pi\lambda x_1/L)}{\sin(\pi\lambda l_1/L)} \\ Y_2(x_2)=\gamma_1\left[\cos(\pi\lambda x_2/L)-\dfrac{\sin(\pi\lambda x_2/L)}{\tan(\pi\lambda l_2/L)}\right]+\gamma_2\dfrac{\sin(\pi\lambda x_2/L)}{\sin(\pi\lambda l_2/L)} \\ Y_3(x_3)=\gamma_2\dfrac{\sin(\pi\lambda x_3/L)}{\sin(\pi\lambda l_3/L)} \end{cases} \tag{7}$$

The force equilibrium equation at the dampers can be written as follows

$$T\left(\left.\frac{\partial u_1}{\partial x_1}\right|_{x_1=l_1}-\left.\frac{\partial u_2}{\partial x_2}\right|_{x_2=0}\right)=-k_1(1+j\phi_1)u_2\big|_{x_2=0} \tag{8}$$

$$T\left(\left.\frac{\partial u_2}{\partial x_2}\right|_{x_2=l_2}+\left.\frac{\partial u_3}{\partial x_3}\right|_{x_3=l_3}\right)=-k_2(1+j\phi_2)u_3\big|_{x_3=l_3} \tag{9}$$

Differentiating the assumed solution in Eqs. (2), (7) and substituting into Eqs. (8), (9) yield

$$\cot(\pi\lambda l_1/L)+\cot(\pi\lambda l_2/L)-\frac{\gamma_2}{\gamma_1}\frac{1}{\sin(\pi\lambda l_2/L)}=-k_1(1+j\phi_1)\frac{L}{\pi\lambda T} \tag{10a}$$

$$-\frac{\gamma_1}{\gamma_2}\frac{1}{\sin(\pi\lambda l_2/L)}+\cot(\pi\lambda l_2/L)+\cot(\pi\lambda l_3/L)=-k_2(1+j\phi_2)\frac{L}{\pi\lambda T} \tag{10b}$$

Define $\Gamma=\pi\lambda$, $\Gamma_n=\pi\lambda l_n/L$ and $\Psi_q=k_q(1+j\phi_q)\dfrac{L}{\pi\lambda T}$. Extracting γ_2/γ_1 from Eq. (10b), substituting into Eq. (10a), yields

$$(\cot\Gamma_1+\Psi_1)(\cot\Gamma_3+\Psi_2)+(\cot\Gamma_1+\Psi_1+\cot\Gamma_3+\Psi_2)\cot\Gamma_2=1 \tag{11}$$

By similarity with a single degree of freedom oscillator (Pacheco *et al*. 1993), ω_i is rewritten as

$$\omega_i=\varpi_i\sqrt{1-\zeta_i^2}+j\zeta_i\varpi_i \tag{12}$$

where ϖ is modulus of the dimensional eigenvalue, ζ is damping ratio and i is mode number. The real and imaginary parts of λ_i can be shown as below

$$\sigma_i=\frac{\varpi_i}{\omega_1^0}\left(\sqrt{1-\zeta_i^2}\right);\quad \varphi_i=\frac{\varpi_i}{\omega_1^0}\zeta_i \tag{13}$$

The modulus of the dimensional eigenvalue ϖ_i and damping ratio ζ_i can be computed from σ_i and φ_i

$$\varpi_i=\sqrt{\sigma_i^2+\varphi_i^2}\,\omega_1^0 \tag{14}$$

$$\zeta_i=\left(\frac{\varphi_i^2}{\sigma_i^2}+1\right)^{-(1/2)} \tag{15}$$

$\cot\Gamma_n$ and Ψ_q can be written explicitly in terms of real and imaginary parts as follows

$$\cot\Gamma_n=A_n-jB_n=\frac{\sin(2\pi\sigma l_n/L)}{\cosh(2\pi\rho l_n/L)-\cos(2\pi\sigma l_n/L)}-j\frac{\sinh(2\pi\rho l_n/L)}{\cosh(2\pi\rho l_n/L)-\cos(2\pi\sigma l_n/L)} \tag{16}$$

$$\Psi_q=C_q+jD_q=\frac{k_qL}{\pi T}\frac{(\sigma+\phi_q\varphi)}{(\sigma^2+\varphi^2)}+j\frac{k_qL}{\pi T}\frac{(\phi_q\sigma-\varphi)}{(\sigma^2+\varphi^2)} \tag{17}$$

Substituting Eqs. (16), (17) into Eq. (11) yields

$$(A_1+C_1)(A_3+C_2)-(-B_1+D_1)(-B_3+D_2)+(A_1+A_3+C_1+C_2)A_2+(-B_1-B_3+D_1+D_2)B_2-1=0 \tag{18}$$

$$(A_1+C_1)(-B_3+D_2)+(-B_1+D_1)(A_3+C_2)-(A_1+A_3+C_1+C_2)B_2+A_2(-B_1-B_3+D_1+D_2)=0 \tag{19}$$

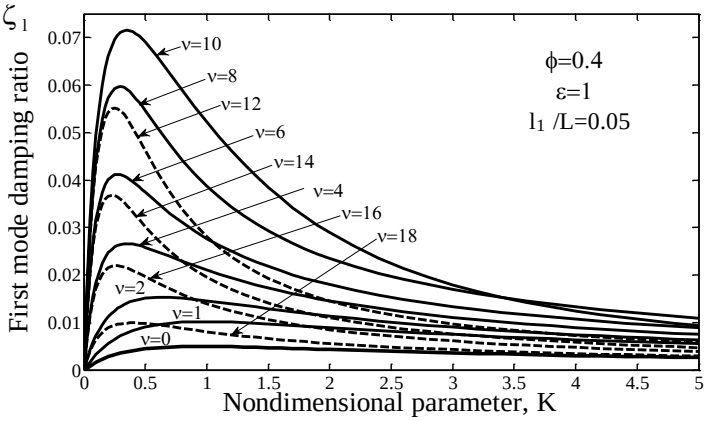

Fig. 2 Relationship between the first mode damping ratio ζ_1 and the nondimensional parameter of the spring factor K for fixed l_1/L=0.05 and variable ν with ε=1, $\phi=\phi_1=\phi_2$=0.4

3. Studying properties of cable–two HDR dampers system

The values of σ_i and φ_i determine the vibration characteristics of the cable-two HDR dampers system; thus it is important to study the oscillation parameters of cable-two HDR dampers system by solving the nonlinear system of Eqs. (18) and (19). In this section, effects of HDR dampers parameters such as damper locations, nondimensional parameter of the spring factors and material loss factor on the dynamic characteristics of the cable are studied in detail by finding exact values of the complex eigenvalue.

The material loss factor of rubber affects the damping ratio of HDR dampers, which is dependent on the hysteresis by both driving frequency and displacement. Natural rubber has a material loss factor range of about 0.01-0.08, and with the development of material technologies, butyl rubber (BR40 and BR60) has a material loss factor ranging from 0.15 up to 0.4 (Marshall and Charney 2010).

3.1 Effects of damper locations

For studying a cable-two HDR dampers system, two nondimensional parameters of the spring factors are introduced as $K_1=k_1l_1/T$ and $K_2=k_2l_3/T$, and two ratios are defined as $\varepsilon=k_2/k_1$ and $\nu=l_3/l_1$. Effects of damper locations on damping ratios are studied for two HDR dampers having the same spring factor (ε=1 leading to $K_2=\nu K_1$) and the same material loss factor ($\phi=\phi_1=\phi_2$=0.4); the first HDR damper is fixed at l_1/L=0.05 while the second one moves so that ν changes from 0 to 18. Relationship between the first mode damping ratio ζ_1 and the nondimensional parameter of the spring factor $K=K_1$ in this case of study is shown in Fig. 2. It is seen that when two dampers are located at the same end of the cable, the damping level is smaller than when two dampers are placed at the opposite ends. For example, when l_1/L=0.05 the damping ratio corresponding to ν=2 is larger than that corresponding to ν=18. Similar observations can be obtained with ν=4 and ν=16; ν=6 and ν=14; ν=8 and ν=12. Therefore, the use of two HDR dampers at the opposite ends of cable is a possible solution.

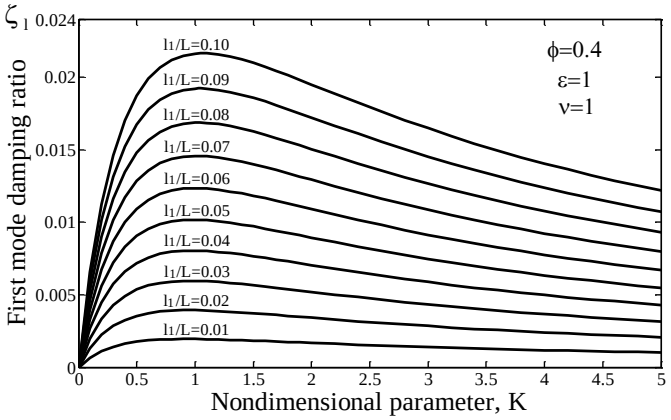

Fig. 3 Relation between the first mode damping ratio ζ_1 and the nondimensional parameter of the spring factor K for variable l_1/L with ε=1, ϕ=0.4 and ν=1

Table 1 The maximum values of the first damping ratios $\zeta_1^{\max}$ and corresponding values of ϖ_1/ω_1^0 for different values of l_1/L with ε=1, ϕ=0.4 and ν=1

	l_1/L	0.010	0.015	0.020	0.025	0.030	0.035	0.040	0.045	0.050	0.06	0.07	0.08	0.09	0.10
Single damper	K^{opt}	0.93	0.94	0.94	0.94	0.94	0.95	0.95	0.95	0.96	0.96	0.97	0.98	0.99	1.00
	$\zeta_1^{\max}$ (%)	0.097	0.146	0.195	0.244	0.294	0.344	0.394	0.444	0.495	0.598	0.702	0.807	0.914	1.023
	$\zeta_1^{\max}/(l_1/L)$	0.097	0.097	0.097	0.098	0.098	0.098	0.098	0.099	0.099	0.100	0.100	0.101	0.102	0.102
	ϖ_1/ω_1^0	1.005	1.008	1.010	1.013	1.015	1.018	1.021	1.023	1.026	1.031	1.037	1.043	1.048	1.054
Two dampers	K^{opt}	0.94	0.94	0.95	0.95	0.96	0.96	0.97	0.98	0.98	1.00	1.01	1.03	1.04	1.06
	$\zeta_1^{\max}$ (%)	0.195	0.293	0.393	0.494	0.596	0.699	0.804	0.910	1.016	1.234	1.458	1.687	1.922	2.164
	$\zeta_1^{\max}/(l_1/L)$	0.195	0.196	0.197	0.198	0.199	0.200	0.201	0.202	0.203	0.206	0.208	0.211	0.214	0.216
	ϖ_1/ω_1^0	1.010	1.015	1.021	1.026	1.031	1.037	1.043	1.048	1.054	1.066	1.078	1.091	1.104	1.118
$\zeta_1^{\max(2HDR)}/\zeta_1^{\max(1HDR)}$		2.010	2.015	2.021	2.026	2.031	2.037	2.042	2.048	2.054	2.065	2.077	2.090	2.103	2.116

3.2 Two symmetric equal dampers are located at opposite ends of the cable

3.2.1 Effects of spring factor and material loss factor on the first mode damping ratio

The HDR dampers are often attached to the cable near the anchorages on opposite ends of the cable. For easy installation and manufacturing of the dampers, the dampers were chosen with the same spring factors k_1=k_2 (ε=1), the same material loss factors ϕ=ϕ_1=ϕ_2 and equal damper locations l_1=l_3=l_d (ν=1), leading to K_1=K_2=K. Effects of the nondimensional parameter of the spring factor K=[0, 5] on the first mode damping ratio ζ_1 for different damper locations l_d/L=[0.01, 0.1] and material loss factors ϕ=0.4 are shown in Fig. 3. Firstly, the damping ratios increase when K increases. After ζ_1 reaches a maximal value, the damping ratios decrease when K increases. Furthermore, the effect of the damper is higher when the relative location of the damper l_d/L is larger.

Table 1 shows maximum values of the first damping ratios $\zeta_1^{\max}$ and corresponding values of

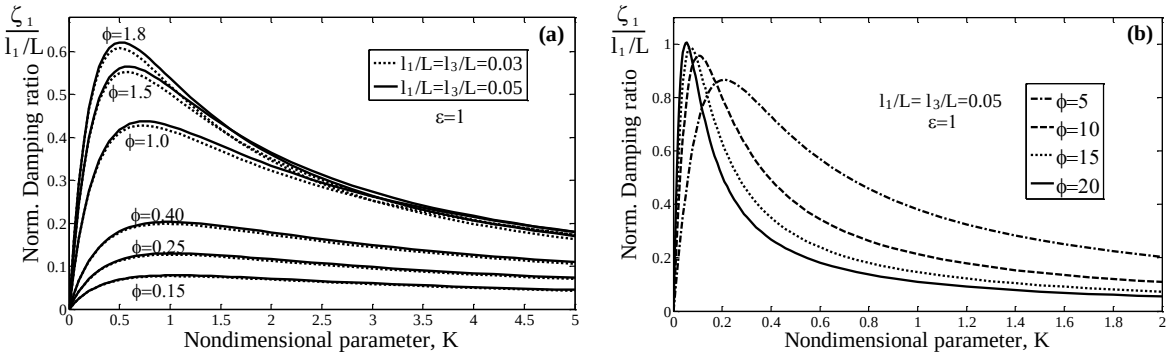

(a) l_1/L=0.03; 0.05 and ϕ=0.15; 0.25; 0.4; 1.0; 1.5; 1.8 (b) l_1/L= 0.05 and ϕ=5; 10; 15; 20

Fig. 4 Relationship between normalized damping ratio $\zeta_1/(l_1/L)$ and the nondimensional parameter of the spring factor K for variable ϕ with ε=1 and ν=1

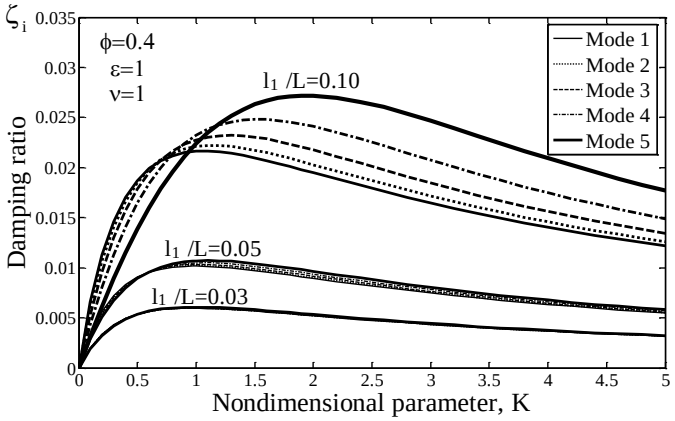

Fig. 5 Relationship between the damping ratio ζ_i and the nondimensional parameter of the spring factor K for variable l_1/L=0.03, 0.05, 0.10 with ε=1, ϕ=0.4 and ν=1

ϖ_1/ω_1^0 with different values of l_1/L for two cases: the cable with a single HDR damper and with two symmetric equal HDR dampers. Table 1 shows that when two HDR dampers are attached at opposite ends of a cable, the maximum damping ratio is approximately double that of a single dampers. This table also shows that the range of maximum normalized damping ratio $\zeta_1^{\max}/(l_1/L)$ is not large, it is [0.097, 0.102] for a single HDR damper and [0.195, 2.16] for two HDR dampers.

The angle δ ranges from 0 for elastic behavior to $\pi/2$ for pure viscous behavior. The loss factor is equal to zero corresponding to no energy dissipated. When the material loss factor ϕ increases, the energy dissipation also increases. While the material loss factor of HDR is about 0.15-0.4 in common practice, a wider range of the material loss factor is considered here to observe the damper behavior. The variation of material loss factor in the range 0.2 to 1.8 was mentioned for a single HDR damper by (Caetano 2007); thus, effects of variable material loss factor (0.15-1.8) on normalized damping ratio $\zeta_1/(l_1/L)$ are shown in the Fig. 4(a). Relationship between normalized damping ratio and the nondimensional parameter of the spring factor for larger values of ϕ is shown in the Fig. 4(b). These figures show that the first mode damping ratios increase when ϕ increases.

Table 2 The maximum damping ratios $\zeta_i^{\max}$ and corresponded values of ϖ_i/ω_1^0 for different values of l_1/L with ε=1, ϕ=0.4 and ν=1

l_1/L	Mode i^{th}	1	2	3	4	5
0.03	K^{opt}	0.96	0.96	0.97	0.98	1.00
	$\zeta_i^{\max}$ (%)	0.596	0.598	0.600	0.603	0.607
	$\zeta_i^{\max}/(l_1/L)$	0.199	0.199	0.200	0.201	0.202
	ϖ_i/ω_1^0	1.031	2.063	3.094	4.126	5.157
0.05	K^{opt}	0.98	1.00	1.02	1.06	1.11
	$\zeta_i^{\max}$ (%)	1.016	1.023	1.034	1.050	1.072
	$\zeta_i^{\max}/(l_1/L)$	0.203	0.205	0.207	0.210	0.214
	ϖ_i/ω_1^0	1.054	2.108	3.162	4.217	5.272
0.10	K^{opt}	1.06	1.14	1.28	1.53	1.94
	$\zeta_i^{\max}$ (%)	2.164	2.221	2.322	2.481	2.718
	$\zeta_i^{\max}/(l_1/L)$	0.216	0.222	0.232	0.248	0.272
	ϖ_i/ω_1^0	1.118	2.238	3.360	4.487	5.620

Fig. 4(b) shows that with larger values of material loss factor, when ϕ increases, ζ_1 reaches a maximal value at smaller valuer of K, and after that, the damping ratios decrease quickly when K increases. When the loss factors are much larger, the maximum normalized damping ratios are equal to about 1.

3.3 Effects of spring factor on damping ratios of different vibration modes

Effects of nondimensional parameter of the spring factor K=[0, 5] on the damping ratios of the first five modes for different damper locations l_d/L = 0.03; 0.05; 0.10 and material loss factor ϕ=0.4 are shown in Fig. 5. The maximum damping ratios $\zeta_i^{\max}$ and corresponding values of ϖ_i/ω_1^0 in this case are shown in Table 2. From Fig. 5 and Table 2 can be seen that when the dampers are installed near the ends of the cable (l_1/L and l_2/L are small), the damping ratios of different vibration modes are similar, but this difference is larger when l_1/L and l_2/L are large. For example, the difference of damping ratio between the first mode and the fifth mode is 1.9% for l_d/L=0.03, 5.4% for l_d/L=0.05, and 25.6% for l_d/L=0.10.

3.4 The change of the oscillation parameters of a cable with two dampers attached

With $\lambda=\sigma+j\varphi$, the vibration solutions can be expressed in the formula

$$u_n(x_n,t)=Y_n(x_n)e^{-\varphi\omega_1^0 t}\left[\cos(\sigma\omega_1^0 t)+j\sin(\sigma\omega_1^0 t)\right] \tag{20}$$

It is seen that φ represents vibration reduction and σ represents vibration. Fig. 6 shows the relationship between ϖ/ω_1^0 and K; and Fig. 7 shows the relationship between ζ_i and ϖ_i/ω_1^0. It is seen that the HDR dampers perturb frequencies of the cable. If $k_1=k_2\to\infty$, $\varphi\to 0$ and $\zeta\to 0$. In this case, the cable vibration vibrates with no displcement at the damper locations. In Fig. 7, the maximum values of ϖ/ω_1^0 corresponds to the frequencies of the longer cable segment of length l_2

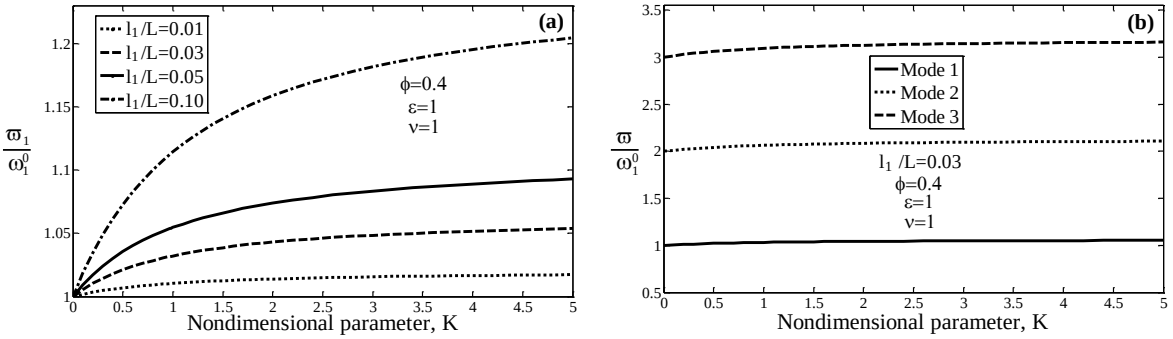

(a) Mode 1 and l_1/L=0.01, 0. 03, 0.05,0.10 (b) Modes 1, 2, 3 and l_1/L=0.03

Fig. 6 Relationship between ϖ_i/ω_1^0 and the nondimensional parameter of the spring factor K with ε=1, ϕ=0.4 and ν=1

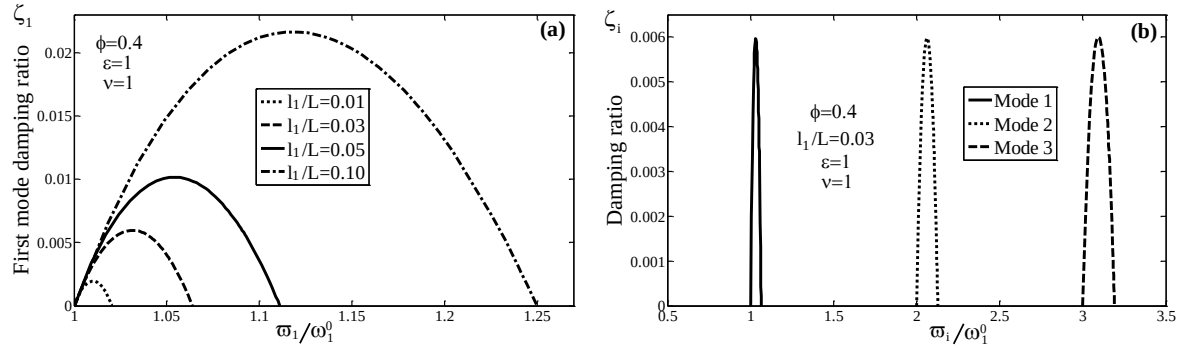

(a) Mode 1 and l_1/L=0.01, 0. 03, 0.05, 0.10 (b) Modes 1, 2, 3 and l_1/L=0.03

Fig. 7 Relationship between the first mode damping ratio ζ_i and ϖ_i/ω_1^0 with ε=1, ϕ=0.4 and ν=1

(σ=iL/l_2 and φ=0). From Table 1 and Table 2 can be seen that the values of ϖ/ω_1^0 corresponding to the maximum normalized damping ratios. These values ϖ/ω_1^0 are larger *i* about 3.1% for l_d/L=0.03, 5.4% for l_d/L=0.05 and 11.8% corresponding to the first mode, 12.4% conrresponding to the fifth mode for l_d/L=0.10. It means that if damper location is near the end of the cable the perturbation is small.

4. Asymptotic formulas

4.1 Asymptotic formulas for two HDR dampers at opposite ends

Eq. (11) can be rewritten as

$$\tan\Gamma=\frac{\left(\Psi_1\sin\Gamma_1\cos\Gamma_3+\Psi_2\cos\Gamma_1\sin\Gamma_3+\Psi_1\Psi_2\sin\Gamma_1\sin\Gamma_3\right)\sin\left(\Gamma_1+\Gamma_3\right)-\left(\Psi_1+\Psi_2\right)\sin\Gamma_1\sin\Gamma_3\cos\left(\Gamma_1+\Gamma_3\right)}{1+\left(\Psi_1\sin\Gamma_1\cos\Gamma_3+\Psi_2\cos\Gamma_1\sin\Gamma_3+\Psi_1\Psi_2\sin\Gamma_1\sin\Gamma_3\right)\cos\left(\Gamma_1+\Gamma_3\right)+\left(\Psi_1+\Psi_2\right)\sin\Gamma_1\sin\Gamma_3\sin\left(\Gamma_1+\Gamma_3\right)} \quad (21)$$

The above examples show that if the dampers are attached near the ends of the cable (l_1/L and l_3/L are both very small), the perturbation in the frequencies of cable is small. Thus, for the first few vibration modes of the cable which are of interest, the $\pi\lambda_i$ of an individual mode i can be assumed to be a small perturbation $\Delta\pi\lambda_i$ from solution of a cable without damper. The tangent can be approximated by

$$\tan(\pi\lambda_i) \cong \pi\lambda_i - i\pi$$

$$\sin(\pi\lambda_i l_1/L) \cong i\pi l_1/L,\ \sin(\pi\lambda_i l_3/L) \cong i\pi l_3/L,\ \sin\left(\pi\lambda_i \frac{l_1+l_3}{L}\right) \cong i\pi \frac{l_1+l_3}{L}$$

$$\cos(\pi\lambda_i l_1/L) \cong 1,\ \cos(\pi\lambda_i l_3/L) \cong 1,\ \cos\left(\pi\lambda_i \frac{l_1+l_3}{L}\right) \cong 1 \tag{22}$$

Substituting the asymptotic Eq. (22) into Eq. (21) yields the asymptotic formula of the solution λ_i

$$\lambda_i \cong i + i\frac{\mathrm{K}_1 l_1/L + \mathrm{K}_2 l_3/L + \mathrm{K}_1\mathrm{K}_2(1-\phi_1\phi_2)(l_1+l_3)/L + j[\phi_1\mathrm{K}_1 l_1/L + \phi_2\mathrm{K}_2 l_3/L + (\phi_1+\phi_2)\mathrm{K}_1\mathrm{K}_2(l_1+l_3)/L]}{1+\mathrm{K}_1+\mathrm{K}_2+\mathrm{K}_1\mathrm{K}_2(1-\phi_1\phi_2)+ j[\phi_1\mathrm{K}_1+\phi_2\mathrm{K}_2+(\phi_1+\phi_2)\mathrm{K}_1\mathrm{K}_2]} \tag{23}$$

The damping ratio ζ_i can be computed from the following approximate formula

$$\begin{aligned}\zeta_i &\cong \frac{\phi_1\mathrm{K}_1\left[\phi_2{}^2\mathrm{K}_2^2+(1+\mathrm{K}_2)^2\right]l_1/L + \phi_2\mathrm{K}_2\left[\phi_1{}^2\mathrm{K}_1^2+(1+\mathrm{K}_1)^2\right]l_3/L}{\left[\phi_1{}^2\mathrm{K}_1^2+(1+\mathrm{K}_1)^2\right]\left[\phi_2{}^2\mathrm{K}_2^2+(1+\mathrm{K}_2)^2\right]} \\ &= \frac{\phi_1\mathrm{K}_1}{\phi_1{}^2\mathrm{K}_1^2+(1+\mathrm{K}_1)^2}(l_1/L) + \frac{\phi_2\mathrm{K}_2}{\phi_2{}^2\mathrm{K}_2^2+(1+\mathrm{K}_2)^2}(l_3/L)\end{aligned} \tag{24}$$

Eq. (24) shows that when two HDR dampers are attached at opposite ends of the cable, the total damping effect is obtained by summing the contributions from single dampers.

For small il_1/L and il_3/L the asymptotic maximum damping ratio can be given

$$\zeta_i^{\max} \cong 0.5\left[\frac{\phi_1}{1+\sqrt{1+\phi_1^2}}\frac{l_1}{L} + \frac{\phi_2}{1+\sqrt{1+\phi_2^2}}\frac{l_3}{L}\right] \quad \text{at } \mathrm{K}_1^{opt} = 1\Big/\sqrt{1+\phi_1^2} \text{ and } \mathrm{K}_2^{opt} = 1\Big/\sqrt{1+\phi_2^2} \tag{25}$$

From Eq. (25) can be seen that the asymptotic maximum damping ratio is determined by the material loss factors, it is quite low for small values of the material loss factor. For example, if $\phi_1=\phi_2=\phi=0.4$ and $\nu=1$, the maximum normalized damping ratios are calculated as $\zeta_i^{\max}/(l_1/L) \cong 0.193$. From Table 1 and Table 2 can be seen that the difference between asymptotic and exact maximum damping ratios. For example, the exact maximum normalized damping ratio is 0.199 for the first mode and 0.202 for the fifth mode with $l_1/L=0.03$, and is 0.203 for the first mode and 0.214 for the fifth mode with $l_1/L=0.05$. When the material loss factor is much larger, the maximum normalized damping ratio is approximately 1 at very small nondimensional parameters (K_1, K_2). This value is similar to the case of the cable with two symmetric equal viscous dampers.

The accurary of the damping ratios calculated by asymptotic formula Eq. (24) can be verified by comparing them with the exact solution. The comparisons are shown in Fig. 8, where the normalized damping ratios of the first mode are plotted versus $K=K_1$ for variable $l_1/L=0.03$, 0.05, 0.10 and $\phi_1=\phi_2=\phi=0.15$, 0.25, 0.4 with $\varepsilon=1$ and $\nu=1$. This figure shows that when l_1/L is small, the

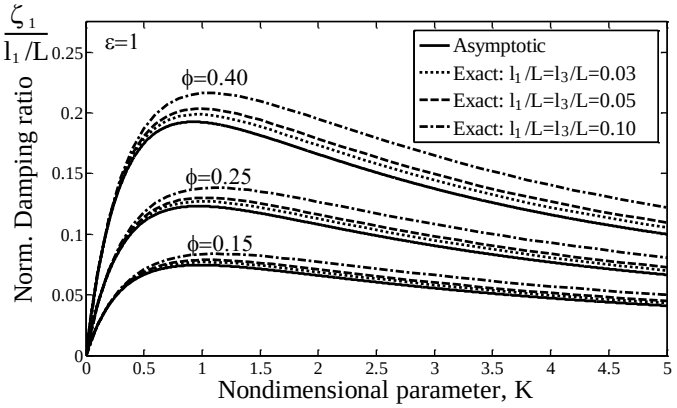

Fig. 8 Comparison of the first mode damping ratios ζ_1 calculated by asymptotic formula with the exact solution for two HDR dampers at opposite ends with ε=1, ν=1 and variable ϕ

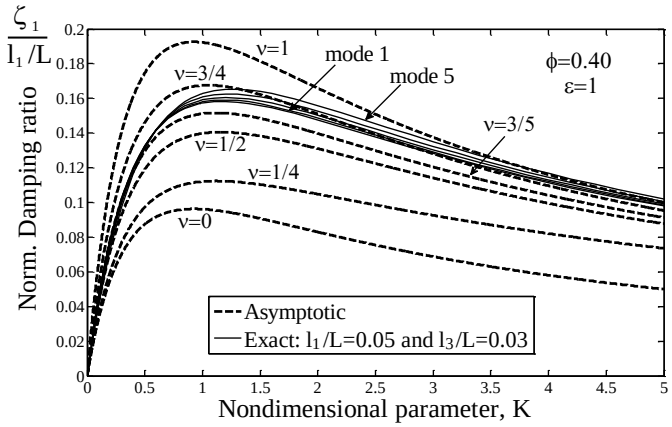

Fig. 9 Family of asymptotic damping curves for different values ν with ε=1 and ϕ= 0.4; and comparison with the exact solution when l_1/L=0.05 and l_3/L=0.03

approximate damping ratios are slightly smaller than the exact values, but this difference is larger when l_1/L is large.

For the purpose of comparing the new asymptotic curves for HDR dampers with existing universal curves for two viscous dampers located in the proximity of the cable ends, Eq. (24) is rewritten for $\phi_1=\phi_2=\phi$, resulting in the following expression which is similar to an equation for two viscous dampers that were derived by Caracoglia and Jones (2007)

$$\frac{\zeta_i}{l_1/L} \cong \frac{\phi K}{(\phi K)^2+(1+K)^2} + \frac{\phi \varepsilon \nu^2 K}{(\phi \varepsilon \nu K)^2+(1+\varepsilon \nu K)^2} \tag{26}$$

Fig. 9 and Fig. 10 are plotted based on Eq. (26) and for the purpose of comparison mentioned above, variables are labeled in a similar way to Caracoglia and Jones (2007). Fig. 9 depicts Eq. (26) as a function of K with ϕ= 0.4 and ε=1 for different values of ν. In this figure, the curves of exact solution for five first modes when l_1/L=0.05 and l_3/L=0.03 are also plotted; therefore they can

compose to asymptotic curve corresponding to ν=3/5. Fig. 9 shows that when ν is incremented the normalized damping curve progressively increases; and when two symmetric equal dampers are located at opposite ends of the cable with ν=1, the corresponding asymptotic curve is at top and its damping ratio is doubled with respect to ν=0. These phenomena are similar to the result of Caracoglia and Jones (2007).

Asymptotic damping curves with ϕ=0.4 for variable ε and three values of $\nu=l_3/l_1$ (1/2, 3/4, 1) are shown in Fig. 10. From Eq. (25) the damping ratio reaches maximum value when K_1 and K_2 are both equal to $1/\sqrt{1+\phi^2}$. Due to $K_1=k_1l_1/T$, $K_2=k_2l_3/T$ and $\nu=l_3/l_1$ then $\varepsilon=k_2/k_1=l_1/l_3=1/\nu$. Therefore, for a given value of ν, the damping ratio reaches maximum values when $\varepsilon=1/\nu$. This phenomenon can be seen from Fig. 10 in which the top of the curves corresponds to $\varepsilon=1/\nu$, which is plotted by solid thick lines.

When compared with the universal curves for viscous dampers by Caracoglia and Jones (2007), Fig. 9 and Fig. 10 show that the damping ratio of HDR dampers is lower than that of viscous dampers. However, for different vibration modes, the damping ratios of HDR dampers are the same while the damping ratios of viscous dampers are different. This means that HDR dampers can provide better vibration reduction to multiple modes.

In a different way, an HDR damper can be considered approximately as a group of a linear spring (k) and a linear dashpot (c^{eq}), which are attached in parallel at the same location. Equivalent viscosities of dashpot can be calculated by asymptotic formulas as follows

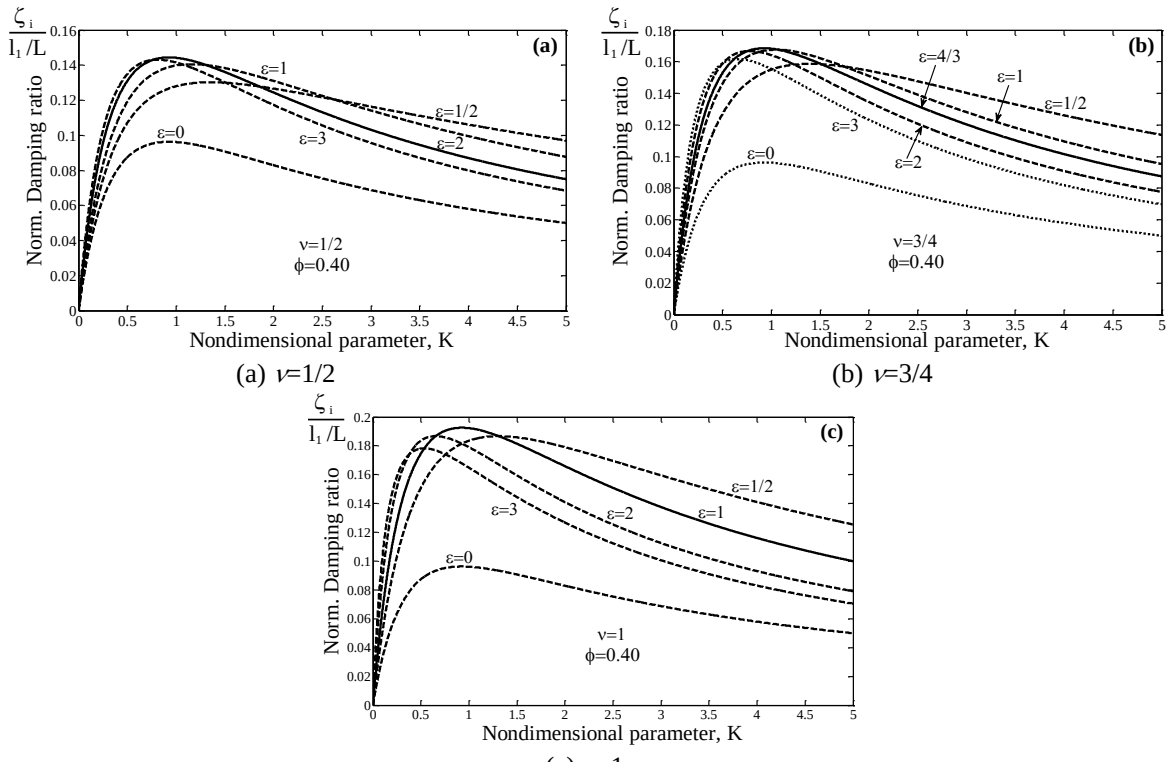

(a) ν=1/2 (b) ν=3/4

(c) ν=1

Fig. 10 Asymptotic damping curves for variable ε and ν

$$c_1^{eq} \cong \frac{k_1\phi_1 L}{i\pi}\sqrt{m/T} \quad \text{and} \quad c_2^{eq} \cong \frac{k_2\phi_2 L}{i\pi}\sqrt{m/T} \tag{27}$$

Based on the study of (Main and Jones 2003), the two damper groups can be considered approximately as two equivalent viscous dampers with effective damper locations given by

$$l_1^{eff} = \frac{l_1}{1+\mathrm{K}_1} \quad \text{and} \quad l_3^{eff} = \frac{l_3}{1+\mathrm{K}_2} \tag{28}$$

Therefore, asymptotic formulas in the papers of Caracoglia and Jones (2007), Hoang and Fujino (2008) can be applied. The damping ratio ζ_i can be computed from the following approximate formula (Hoang and Fujino 2008)

$$\zeta_i \cong \frac{i\pi\eta_1^{eq}\left(l_1^{eff}/L\right)}{1+\left[i\pi\eta_1^{eq}\left(l_1^{eff}/L\right)\right]^2}\frac{l_1^{eff}}{L} + \frac{i\pi\eta_2^{eq}\left(l_3^{eff}/L\right)}{1+\left[i\pi\eta_2^{eq}\left(l_3^{eff}/L\right)\right]^2}\frac{l_3^{eff}}{L} \tag{29}$$

where $\eta_1^{eq} = \frac{c_1^{eq}}{\sqrt{Tm}} \cong k_1\phi_1\frac{L}{i\pi T}$ and $\eta_2^{eq} = \frac{c_2^{eq}}{\sqrt{Tm}} \cong k_2\phi_2\frac{L}{i\pi T}$ are nondimensional parameters of equivalent viscous dampers.

Eq. (29), which is consistent with Eq. (24), shows that for each vibration mode an HDR damper is equivalent to a viscous damper. These asymptotic formulas also show that the HDR damper is different from other types of damper by the fact that its asymptotic universal curves do not depend on mode. Additionally, when K_1 and K_2 are very small and ϕ_1, ϕ_2 are very large, Eq. (28) leads to $l_1^{eff} \cong l_1$ and $l_3^{eff} \cong l_3$, meaning that in this case for a given mode two HDR dampers are equivalent to two viscous dampers that are installed at l_1 and l_3.

4.2 Asymptotic formulas for two HDR dampers at the same end

When two HDR dampers are located near the anchorage at the same end of the cable, two nondimensional parameters of the spring factors are introduced: $K_1=k_1l_1/T$ and $\overline{\mathrm{K}}_2=k_2(l_1+l_2)/T$. Eq. (11) can be rewritten as

$$\tan\Gamma = \frac{\left[\Psi_2\cos\Gamma_1\sin\Gamma_2 + \Psi_1\Psi_2\sin\Gamma_1\sin\Gamma_2 + (\Psi_1+\Psi_2)\sin\Gamma_1\cos\Gamma_2\right]\sin(\Gamma_1+\Gamma_2) - \Psi_1\sin\Gamma_1\sin\Gamma_2\cos(\Gamma_1+\Gamma_2)}{1+\left[\Psi_2\cos\Gamma_1\sin\Gamma_2 + \Psi_1\Psi_2\sin\Gamma_1\sin\Gamma_2 + (\Psi_1+\Psi_2)\sin\Gamma_1\cos\Gamma_2\right]\cos(\Gamma_1+\Gamma_2) + \Psi_1\sin\Gamma_1\sin\Gamma_2\sin(\Gamma_1+\Gamma_2)} \tag{30}$$

Given that two HDR dampers are attached very close to the end of the cable and only the first few modes of cable vibration are of interest, applying the asymptotic approximations for very small values of l_1/L and l_2/L yields the asymptotic formula of the solution λ_i

$$\lambda_i = i + i\frac{l_1+l_2}{L}\frac{\mathrm{K}_1 l_1/(l_1+l_2) + \overline{\mathrm{K}}_2 + (1-\phi_1\phi_2)\mathrm{K}_1\overline{\mathrm{K}}_2 l_2/(l_1+l_2) + j\left[\phi_1\mathrm{K}_1 l_1/(l_1+l_2) + \overline{\mathrm{K}}_2 + (\phi_1+\phi_2)\mathrm{K}_1\overline{\mathrm{K}}_2 l_2/(l_1+l_2)\right]}{1+\mathrm{K}_1+\overline{\mathrm{K}}_2 + (1-\phi_1\phi_2)\mathrm{K}_1\overline{\mathrm{K}}_2 l_2/(l_1+l_2) + j\left[\phi_1\mathrm{K}_1 + \overline{\mathrm{K}}_2 + (\phi_1+\phi_2)\mathrm{K}_1\overline{\mathrm{K}}_2 l_2/(l_1+l_2)\right]} \tag{31}$$

In this case, approximate formula for the calculation of the damping ratio ζ_i is expressed as follows

$$\frac{\zeta_i}{(l_1+l_2)/L} = \frac{\phi_1\mathrm{K}_1 l_1/(l_1+l_2) + \phi_2\overline{\mathrm{K}}_2 + 2\phi_2\mathrm{K}_1\overline{\mathrm{K}}_2 l_2/(l_1+l_2) + \phi_2\left(1+\phi_1^2\right)\mathrm{K}_1^2\overline{\mathrm{K}}_2 l_2^2/(l_1+l_2)^2}{\left[1+\mathrm{K}_1+\overline{\mathrm{K}}_2 + (1-\phi_1\phi_2)\mathrm{K}_1\overline{\mathrm{K}}_2 l_2/(l_1+l_2)\right]^2 + \left[\phi_1\mathrm{K}_1 + \phi_2\overline{\mathrm{K}}_2 + (\phi_1+\phi_2)\mathrm{K}_1\overline{\mathrm{K}}_2 l_2/(l_1+l_2)\right]^2} \tag{32}$$

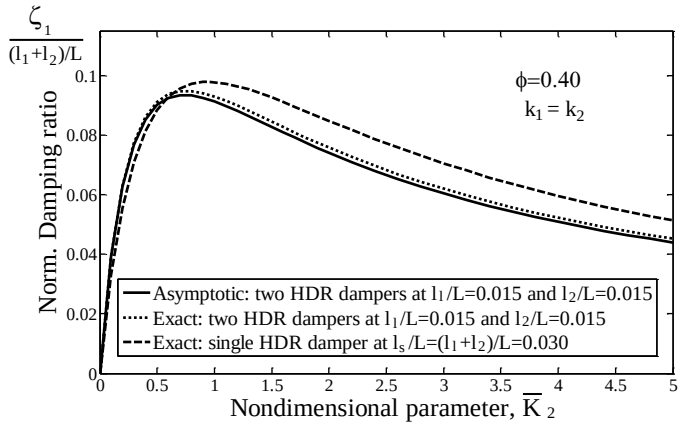

Fig. 11 Comparison of the first mode damping ratios ζ_1 calculated by asymptotic formula with the exact solution for two HDR dampers at the same end with $l_1/L = l_2/L$=0.015, k_1=k_2 and ϕ=0.4

A comparison of the damping ratios which are calculated by asymptotic formula in Eq. (32) with the exact solution is shown in Fig. 11, where the normalized damping ratios of the first mode are plotted versus $\overline{K}_2$ for l_1/L=l_2/L=0.015 and k_1=k_2 with ϕ_1=ϕ_2=ϕ=0.4. The first mode damping ratios ζ_1 when two dampers are installed at the same end of the cable can be compared with a single damper when it is attached at the same location of the second damper in the former case: l_s=(l_1+l_2)/L=0.03. When l_1/L and l_2/L are small, the approximate damping ratios are slightly smaller than the exact values. This figure also compares the damping ratios in two cases: two dampers and one damper; the damper in the latter case is at the same location of the second damper in the former case. At small values of K, the damping ratio of two dampers is only slightly larger than that of one damper. At larger values of K, the damping ratio of two dampers is even smaller. This means that two dampers that are installed close to each other are not efficient. This result agrees with the studies by Main and Jones (2003), Caracoglia and Jones (2007), Hoang and Fujino (2008).

5. Design example of HDR dampers for stay cable

HDR dampers are designed to reduce the rain-wind induced vibrations of stay cable with parameters as follows: length of cable L=110 m; cable diameter D=0.16 m; cable mass per unit length m=61.4 kg/m; tension in the cable T=5000 kN and air density ρ=1.23 kg/m^3. Natural frequency of the first mode $f_1^0 = 1.3$Hz.

To avoid rain-wind induced vibrations, the stability criterion was proposed by (PTI 2001) for a smooth circular cable

$$\zeta > \frac{10\rho D^2}{m} \tag{33}$$

where m is mass per unit length; ζ is damping ratio; ρ is air density and D is cable diameter.

Using the cable parameters above yields ζ>0.513%. If one HDR damper with material loss factor of 0.4 is used, it needs to be placed at least 5.7 m from the cable end and nondimensional parameter of the spring factor of 0.96 is chosen to achieve a maximum damping ratio of 0.513%.

Table 3 Design of HDR dampers for vibration reduction of the cable

	Exact Solution			Asymptotic Solution		Difference (%)
	σ_i	$\varphi_i \times 10^{-2}$	ϖ_i/ω_1^0	ζ_i (%)	ζ_i (%)	
Mode 1	1.0236	0.5382	1.0236	0.5257	0.5134	2.34
Mode 2	2.0471	1.0774	2.0471	0.5263	0.5134	2.45
Mode 3	3.0703	1.6187	3.0703	0.5272	0.5134	2.62
Mode 4	4.0931	2.1632	4.0932	0.5285	0.5134	2.86
Mode 5	5.1154	2.7115	5.1155	0.5301	0.5134	3.15

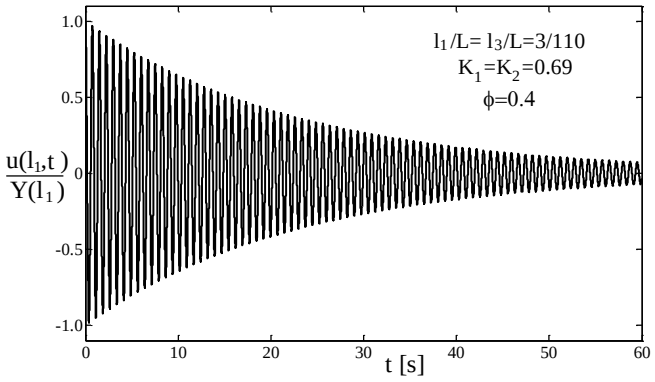

Fig. 12 Free vibration of the cable at the first damper location in the design example ($l_1/L=l_3/L$=3/110, $K_1=K_2$=0.69 and ϕ=0.4)

However, this location is hard to install damper. Due to geometric constraints, the distance between the anchorage and the damper is required not greater than 3m. To satisfy this requirement, two HDR dampers are proposed to install at opposite ends of the cable with $l_1=l_3$=3 m (ν=1). The two symmetric equal HDR dampers are chosen with the same spring factors ($\varepsilon=k_2/k_1$=1) and material loss factor ($\phi_1=\phi_2=\phi$=0.4). To achieve the damping ratio ζ=0.513%, from Eq. (24) the nondimensional parameters of the spring factors $K=K_1=K_2$=0.69 were calculated, leading to the spring factors $k_1=k_2$=1150kN/m. The oscillation parameters of the cable-dampers system are shown in Table 3; and free vibration of the cable at the first damper location is shown in Fig. 12.

6. Conclusions

In this paper, the general dynamic characteristics of cable-two HDR dampers system investigated by modeling the stay cable as a taut string and each HDR damper as complex-valued impedance with spring factor (k) and material loss factor (ϕ). Effects of different parameters on vibration reduction were analyzed in detail using an analytical formulation of the complex eigenvalue problem. The relationships between the damping ratio and locations of the dampers, the spring factors, and the material loss factors were studied and plotted in figures. Additionally, asymptotic formulas were proposed for the calculation of damping ratios of the cable-two HDR dampers system and the accuracy of the damping ratios as calculated by the asymptotic formulas was also

compared with the exact solutions. From these studies, the following conclusions can be drawn:

• When two HDR dampers are attached at opposite ends of a cable, the total damping ratio is the approximate sum of contributions from single dampers. In the contrast, when two HDR dampers are installed at the same end of the cable, due to interaction between the two dampers, the damping ratio is lower than when one HDR damper is used. Therefore, use of two HDR dampers at the opposite ends of the cable is a possible solution, it corresponds to higher damper levels.

• If HDR dampers are installed near the ends of the cable the values of damping ratios of different vibration modes are similar; thus in this case, the HDR dampers can provide the same level of vibration reduction to multiple modes.

• The effect of the material loss factor (ϕ=tanδ) of the HDR dampers on the damping ratio (ζ) of the cable is extremely important. The angle δ ranges from 0 for elastic behavior to $\pi/2$ for pure viscous behavior. The loss factor is equal to zero corresponding to no energy dissipated. When the material loss factor ϕ increases, the energy dissipation increases; thus the damping ratio also increases.

• In designing dampers for cable vibration reduction, it is necessary to determine the levels of supplemental damping provided in the first several modes of vibration for different values of the damper parameters and different damper locations. Due to geometric constrants, the dampers are often attached to the cable near the anchorages. When the HDR damper is installed at such a location the perturbation in the frequencies of cable is very small; thus, the approximate formulas Eqs. (24)-(26) and Eq. (32) can be are useful for designing process.

• Although damping ratio of an HDR damper is not as high as that of other damper types such as viscous damper, it has many advantages such as compact size, better aesthetics, easy maintenance, temperature stability, cost benefits, and can provide better vibration reduction to multiple modes. HDR dampers are particularly suitable for relatively short stay cables. For longer cables, the damping of the cable can be improved by use of two HDR dampers attached at opposite ends of a cable.

Based on the findings of this study, one can choose the optimal parameters of the HDR dampers for a given cable.

Acknowledgments

The authors of this paper would like to acknowledge the support of The China Transportation Construct Science and Technology Program (2011318223170). The authors also express sincere appreciation to the reviewers for a careful reading of the manuscript and for raising valuable comments to improve this paper.

References

Bert, C.W. (1973), "Material damping: An introductory review of mathematic measures and experimental technique", *J. Sound Vib.*, **29**(2), 129-153.

Caracoglia, L. and Jones, N.P. (2007), "Damping of taut-cable systems: two dampers on a single stay", *J. Eng. Mech.*, **133**(10), 1050-1060.

Caetano, E. (2007), *Cable vibrations in cable-stayed bridges*, Structural Engineering Documents, SED 9, IABSE-AIPC-IVBH, Zurich, Switzerland.

Freyssinet (2005), BaiChay Bridge in Vietnam: Internal dampers - Efficiency estimation & Stay vibration analysis.
Fujino, Y. and Hoang, N. (2008), "Design formulas for damping of a stay cable with a damper", *J. Struct. Eng.*, **134**(2), 269-278.
Fujino, Y., Kimura, K. and Tanaka, H. (2012), *Cable Vibrations and Control Methods*, In Wind Resistant Design of Bridges in Japan, Springer Japan.
Wenzel, H. and Tanaka, H. (2006), *Samco Monitoring glossary*, Vienna Consulting Engineers Holding GmbH, Vienna, Austria.
Hikami, Y. and Shiraishi, N. (1988), "Rain-wind induced vibrations of cables stayed bridges", *J. Wind Eng. Indus. Aerod.*, **29**(1), 409-418.
Hoang, N. and Fujino, Y. (2008), "Combined damping effect of two dampers on a stay cable", *J. Bridge Eng.*, **13**(3), 299-303.
Huang, Z. and Jones, N.P. (2011), "Damping of taut-cable systems: Effects of linear elastic spring support", *J. Eng. Mech.*, **137**(7), 512-518.
Jung, S.S., Kim, Y.T., Lee, Y.B., Shin, S.H., Kim, D. and Kim, H.C. (2006), "Measurement of the resonance frequency, the loss factor, and the dynamic young's modulus in structural steel and polycarbonate by using an acoustic velocity sensor", *J. Korean Phys. Soc.*, **49**(5), 1961-1966.
Krenk, S. (2000), "Vibrations of a taut cable with an external damper", *J. Appl. Mech.*, **67**(4), 772-776.
Kumarasena, S., Jones, N.P., Irwin, P. and Taylor, P. (2007), *Wind-induced vibration of stay cables*, Federal Highway Administration, Publication No. FHWA-RD-05-083.
Main, J.A. and Jones, N.P. (2002a), "Free vibrations of taut cable with attached damper. I: Linear viscous damper", *J. Eng. Mech.*, **128**(10), 1062-1071.
Main, J.A. and Jones, N.P. (2002b), "Free vibrations of taut cable with attached damper. II: Nonlinear damper", *J. Eng. Mech.*, **128**(10), 1072-1081.
Main, J.A. and Jones, N.P. (2003), "Influence of rubber bushings on stay cable damper effectiveness", *Proceedings of the Fifth International Symposium on Cable Dynamics*, Santa Margherita Ligure, Italy.
Marshall, J.D. and Charney, F.A. (2010), "A hybrid passive control device for steel structures, I: Development and analysis", *J. Constr. Steel Res.*, **66**(10), 1278-1286.
Matsumoto, M., Shirashi, N. and Shirato, H. (1992), "Rain-wind induced vibration of cables of cable-stayed bridges", *J. Wind Eng. Indus. Aerod.*, **44**, 2011-2022.
Nakamura, A., Kasuga, A. and Arai, H. (1997), "The effects of mechanical dampers on stay cables with high-damping rubber", *Constr. Build. Mater.*, **12**(2), 115-123.
Pacheco, B., Fujino, Y. and Sulekh, A. (1993), "Estimation curve for modal damping in stay cables with viscous damper", *J. Eng. Mech.*, **119**(6), 1961-1979.
PTI Guide Specification (2001), *Recommendations for stay cable design, testing and installation*, Fourth Edition, Post-Tensioning Institute Committee on Cable-Stayed Bridges.
Takano, H., Ogasawara, M., Ito, N., Shimosato, T., Takeda, K. and Murakami, T. (1997), "Vibrational damper for cables of the Tsurumi Tsubasa Bridge", *J. Wind Eng. Indus. Aerod.*, **69-71**, 807-818.
Zhou, H., Sun, L. and Xing, F. (2014), "Free vibration of taut cable with a damper and a spring", *Struct. Control Hlth. Monit.*, **21**(6), 996-1014.

CC